

# Multilevel edge detection using quantum and classical genetic algorithms: A comparative study

S.Khalek,<sup>1,2,\*</sup> A. Ben Ishak,<sup>3</sup> and A.-S. F. Obada<sup>2</sup>

<sup>1</sup>International Centre for Theoretical Physics, Strada Costiera, Italy.

<sup>2</sup>Mathematics Department, Faculty of Science, Al-Azhar University, Cairo, Egypt.

<sup>3</sup>Universit de Tunis, ISGT, LR99ES04 BESTMOD, 2000, Le Bardo, Tunisia.

## Summary

In this work, we develop a multilevel edge detection method based on the Kapur and Tsallis entropies. The multilevel thresholding approach gives rise to an NP-hard optimization problem. We have used the Classical Genetic Algorithm (CGA) and the Quantum Genetic Algorithm (QGA) to solve this problem. The performance of the QGA has been tested on ten sample images and it is shown that the QGA outperforms significantly the CGA on a sample of real-world images. Moreover, it was found that the Kapur entropy leads to a slightly better image segmentation quality than the Tsallis one.

### Keywords:

*Quantum genetic algorithm; genetic algorithm; Multilevel thresholding; Edge detection; Tsallis entropy; Kapur entropy. PACS numbers:*

## 1. Introduction

Digital image processing is one of the most applicable research areas used in many practical applications in different fields like medicine, security, quality control, astronomy, etc. Image segmentation is one of the most widely used image processing techniques. The goal of image segmentation is to divide an image into homogeneous and disjoint sets of pixels sharing similar properties such as intensity, color or contours. Image segmentation usually represents the first step in image understanding. The results obtained by segmentation are used for further higher-level methods such as feature extraction, semantic interpretation, image recognition, and classification of objects [1].

Image thresholding is a largely used segmentation technique that performs image segmentation based on the information contained in the image histogram. In the literature we found a lot of image processing applications including medical image analysis, automatic target recognition, infrared gait recognition, optical character recognition, etc. Thresholding is a widely used technique in various image processing applications. In general, thresholding approaches are divided into parametric and nonparametric methods.

The nonparametric family of approaches search for the optimal thresholding values that separate the gray-level regions of an image according to some discriminating criteria like the between class variance and the maximum entropy thresholding. However, in the parametric approaches the gray-level distribution of each group is assumed to obey a Gaussian distribution. The goal is to estimate the parameters of Gaussian distribution that best fits the histogram [2].

Nonparametric thresholding can be divided into bilevel and multilevel thresholding. Bilevel thresholding classifies the pixels into two groups (object and background), one including those pixels with gray levels above a certain threshold and the other including the rest. Multilevel thresholding divides the pixels into several classes. The pixels belonging to the same class have gray levels within a specific range defined by several thresholds.

Generally, the multilevel image thresholding problem is transformed into an optimization problem. Indeed, the optimal thresholds are obtained by getting the optimum of an objective function based on the image informations. Presumably, the objective functions based on the entropy (Kapur method) and the between-class variance (Otsu method) are the most popular ones [1].

Nondeterministic metaheuristic optimization and digital image processing are two very different research fields, both extremely active and applicable. They touch in a very limited area, but that narrow interaction opens new very promising applications for digital image processing and new and different deployment of metaheuristic optimization. More specifically, in image processing some hard optimization problems occur. For example, multilevel image thresholding is an NP-hard combinatorial problem. Indeed, it consists in finding  $k$  optimal numbers in the image intensities range  $[0, 255]$ . Such problem cannot be solved in reasonable time by standard mathematical deterministic methods. For instance, an exhaustive search for 4 thresholding values for Lena image is computationally prohibitive.

Meanwhile, the computation time will increase exponentially with the number of thresholds. Consequently, Nature inspired metaheuristic algorithms have recently been successfully used for this type of hard optimization problems to find acceptable sub-optimal thresholds quickly. In this work we choose to compare the Quantum Genetic Algorithm to the Classical Genetic Algorithm to determine the thresholding values. We will also compare the Kapur and the Tsallis entropies.

The remainder of this paper is organized as follows. The next section describes the used heuristics and entropies. The multilevel edge detection approach is presented in section 3. The experimental results are given in section 4. Finally, Section 5 is devoted to some concluding remarks and presents some possible perspectives.

## 2. Genetic Algorithms for Image Processing

Multilevel image thresholding is very important for image segmentation, which in turn is crucial for higher level image analysis. A proper segmentation is heavily dependent on adequately computed thresholds. The problem includes exponential combinatorial optimization with complex objective functions which are efficiently solvable only by nondeterministic methods [3].

Best possible thresholds (absolute optimum) can always be found by exhaustive search. All possibilities can be examined and the best one selected. However, the number of possibilities when searching for  $k$  thresholds within the range  $[0, 255]$

is  $C(255, k) = \frac{255!}{k!(255-k)!}$ . Since computational time for finding multiple thresholds grows exponentially with the number of desired thresholds, the exhaustive search is not a reasonable option. However, the intelligence nondeterministic metaheuristics based on evolutionary computation offer an interesting alternative to the exhaustive search.

In this section we present the classical and the quantum genetic algorithms that we will use in our experiments.

### A. Classical genetic algorithm

Many algorithms are performed to multilevel thresholding segmentation to improve the computational efficiency. Genetic algorithm (GA) provides a common system framework to solve complex optimization problems, and independent on the specific problem areas.

The father of the original Genetic Algorithm (GA) was John Holland [4] who invented it in the early 1970's.

the traditional exhaustive method does not work.

Genetic algorithms belong to the larger class of Evolutionary Algorithms (EA),

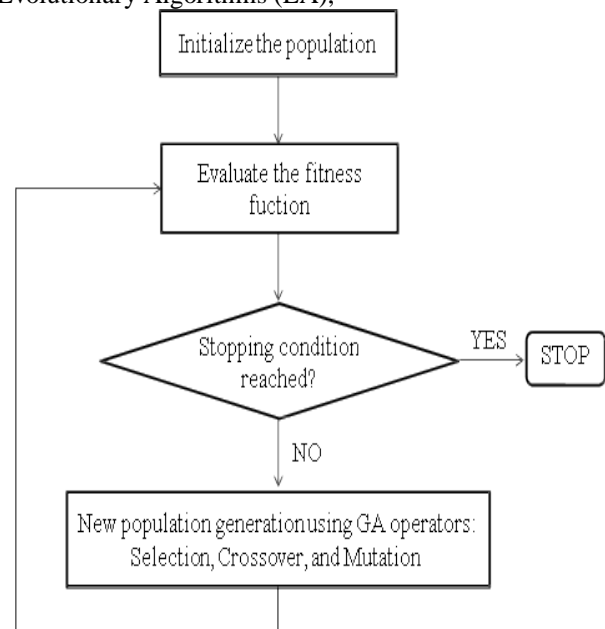


FIG. 1: Genetic algorithm flowchart.

which generate solutions to optimization problems using techniques inspired by natural evolution. A GA comes from the artificial intelligence field and it is an adaptive heuristic search algorithm that mimics some of the processes observed in natural selection.

An implementation of a GA begins with a population of chromosomes (typically random). One then evaluates these structures and allocates reproductive opportunities in such a way that those chromosomes which represent a better solution to the target problem are given more chances to "reproduce" than those chromosomes which are poorer solutions. The "goodness" of a solution is typically defined with respect to the current population [5].

In the computational sense, the main operators of a GA are evaluation, selection, crossover and mutation. Given a clearly defined problem to be solved and a bit-string representation for candidate solutions, the simple GA works as shown in figure 1.

The main advantages of GA are as follows:

- It is derivative-free technique.
- It can be used for both continuous and discrete optimization problems.
- It uses stochastic operators instead of deterministic rules to search for an optimum solution. It considers many

points in the search space simultaneously, not a single point. Thus, there is a reduced chance of converging to local minima.

- It works directly with binary strings of characters representing the parameter set (population, solution set), but not the parameters themselves.

In our image segmentation problem we aim at dividing the pixels into two groups that maximizes the Tsallis and Kapur entropies which are employed as fitness functions.

B. Quantum genetic algorithm

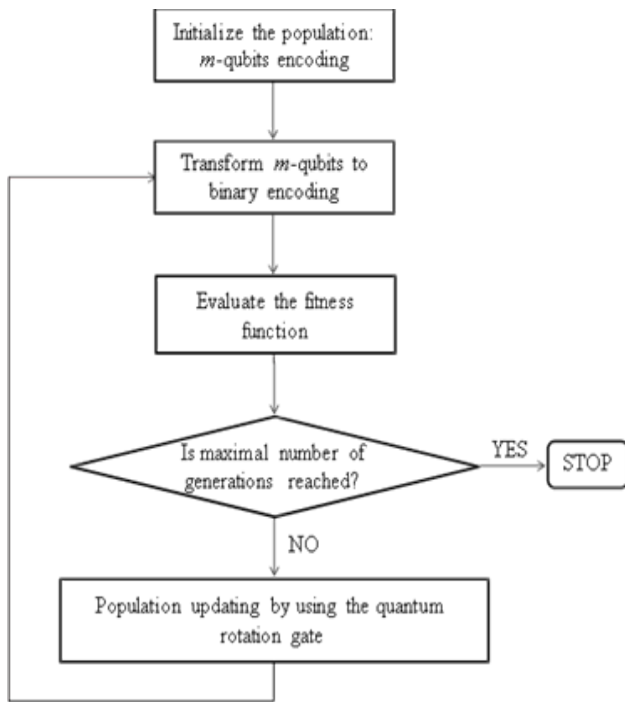


FIG. 2: Quantum genetic algorithm flowchart.

QGA is proposed in the framework of a qubit and quantum superposition state [6, 7, 8, 9]. Qubit is the main unit of information in quantum computers. It is acts any state  $|0\rangle$ ,  $|1\rangle$ , or any superposition state between them [10]. A state of a qubit can be written as

$$|\psi\rangle = \alpha|0\rangle + \beta|1\rangle$$

where  $\alpha, \beta$  are complex numbers satisfy the normalization

condition  $|\alpha|^2 + |\beta|^2 = 1$ . The states  $|0\rangle(|1\rangle)$  are the spin up (down) respectively. In this way the multiqubits can be encoded as

$$Q^j = \begin{matrix} & 11 & 12 & \dots & 1r & 21 & 22 & \dots & 2r & m1 & m2 & \dots & mr \\ j & \beta^t & \beta^t & \dots & \beta^t & \beta^t & \beta^t & \dots & \beta^t & \beta^t & \beta^t & \dots & \beta^t \end{matrix}$$

Where  $Q^j$  represents the  $j$ th individual chromosome of the  $j$ th generation;  $m$  represents the number of qubits encoding of each gene;  $t$  represents the number of genes in the chromosome [11]. Let us consider the quantum encoding for the amplitudes  $(\alpha, \beta)$  for each individual in the population with  $(1, 1)$  which indicates that when  $t = 0$ , the possibility of each state expressed by a chromosomal is equal [12].

$$\begin{matrix} \sqrt{2} & \sqrt{2} \\ 2 & 2 \end{matrix}$$

Quantum Rotating Gates (QRG) compared with the conventional GA, QGA applies the probability amplitude of qubits to encode chromosome and uses QRG to realize chromosomal updated operation. Since the chromosomes are prepared in the entanglement state or in the superposition state, so the generation of offspring can not be determined by the parent group when the QRG is used to realize the genetic operation. It is jointly detected by the optimal individual of the parent group and probability amplitude of each qubit. In this way, the genetic manipulation of QGA is mainly through acting on the entanglement state by the QRG to change the probability amplitude. Therefore, the construction of QRG is the key issue of QGA [13, 14] and it directly affects the performance of the algorithm.

The QRG can be defined as

$$U(\varphi_j) = \begin{pmatrix} \cos \varphi_j & -\sin \varphi_j \\ \sin \varphi_j & \cos \varphi_j \end{pmatrix}$$

The updated process is

$$\begin{pmatrix} \alpha_j^1 \\ \beta_j^1 \end{pmatrix} = U(\varphi_j) \begin{pmatrix} \alpha_j \\ \beta_j \end{pmatrix} = \begin{pmatrix} \cos \varphi_j & -\sin \varphi_j \\ \sin \varphi_j & \cos \varphi_j \end{pmatrix} \begin{pmatrix} \alpha_j \\ \beta_j \end{pmatrix}$$

Table 1: Adjustment strategy of rotating angle.

| $x_j$ | $best_j$ | $f(x) > f(best)$ | $\Delta\phi_j$     | $s(\alpha_j, \beta_j)$ |                       |                            |
|-------|----------|------------------|--------------------|------------------------|-----------------------|----------------------------|
|       |          |                  |                    | $\alpha_j\beta_j > 0$  | $\alpha_j\beta_j < 0$ | $\alpha_j = 0 \beta_j = 0$ |
| 0     | 0        | False            | 0                  | 0                      | 0                     | 0                          |
| 0     | 0        | True             | 0                  | 0                      | 0                     | 0                          |
| 0     | 1        | False            | $\Delta\phi_j + 1$ | -1                     | 0                     | $\pm 1$                    |
| 0     | 1        | True             | $\Delta\phi_j - 1$ | +1                     | $\pm 1$               | 0                          |
| 1     | 0        | False            | $\Delta\phi_j - 1$ | +1                     | $\pm 1$               | 0                          |
| 1     | 0        | True             | $\Delta\phi_j + 1$ | -1                     | 0                     | $\pm 1$                    |
| 1     | 1        | False            | 0                  | 0                      | 0                     | 0                          |
| 1     | 1        | True             | 0                  | 0                      | 0                     | 0                          |

where  $(\alpha_j, \beta_j)^T$  and  $(\alpha_l, \beta_l)^T$  are the probability amplitudes of the  $r$ th qubit in chromosome before and after the QRG updating. Also,  $\phi_j$  are given in Table 1 to determined the value and the sign of  $\phi_j$  [15]. Moreover,  $x_i$  is the  $j$ th bit of the current chromosome;  $best_j$  is the  $j$ th bit of the current optimal chromosome. Also,  $\Delta\phi_j$  is the value of the rotating angle,  $f(x)$  is the fitness function which we consider it as the Reyni and Tasslis entropy. On the other hand  $s(\alpha_j, \beta_j)$  is the direction of the rotating angle and . The value of  $\Delta\phi_j$  is determined by a certain adjustment strategy, in conventional QGA and the value of  $\Delta\phi_j$  is generally a constant value is around  $0.01\pi$ . The adjustment strategy is, comparing the fitness of the currently measured value  $\Delta\phi_j$  of the individual  $f(x)$  with the fitness of the current optimal individual  $f(best_j)$ , if  $f(x) > f(best)$ , then adjust the corresponding qubits of  $Q_t$ , making the probability amplitude  $(\alpha_j, \beta_j)$  evolves toward the direction that is propitious to the emergence of  $x_j$ . Conversely, if  $f(x) < f(best)$ , then adjust the corresponding qubits of  $Q_t$ , making the probability amplitude  $(\alpha_j, \beta_j)$  evolves toward the direction that is propitious to the emergence of best

#### A. Tsallis and Kapur entropies

The entropy is basically a thermodynamic concept associated with the order of irreversible processes from a traditional point of view. In this regard Shannon redefined the entropy concept of Boltzmann/Gibbs as a measure of uncertainty regarding the information content of a system [16]. The Shannon entropy is defined from the probability distribution, where  $p_k$  denotes the

probability of each state  $j$ . Therefore, the Shannon entropy is defined as:

$$S_H = - \sum_{k=1}^L p_k \log p_k \quad (1)$$

where  $L$  is the total number of states or symbols. For a two statistical independent subsystems  $A$  and  $B$ , the Shannon entropy satisfies the extensive property (additivity):

$$S(A + B) = S(A) + S(B) \quad (2)$$

However, for a certain class of physical system which entail long-range interactions, long time memory, and fractal-type structures, it is necessary to use nonextensive entropy. Tsallis has proposed a generalization of BGS statistics, and its form can be depict

$$S_q = \frac{1 - \sum_{k=1}^q (p_k)^q}{q - 1}$$

where the real number  $q$  denotes an entropic index that characterizes the degree of nonextensivity.

Above expression will meet the Shannon entropy in the limit  $q \rightarrow 1$ . The Tsallis entropy is nonextensive in such a way that for a statistical dependent system. Its entropy is defined with the obey of pseudo additivity rule:

$$S_q(A + B) = S_q(A) + S_q(B) + (1 - q)S_q(A)S_q(B)$$

It is well known that three different entropies can be defined with regard to different values of q. For q < 1 the Tsallis entropy becomes a subextensive entropy where Sq (A+B) < Sq (A)+Sq (B); for q = 1, the Tsallis entropy reduces to an standard extensive entropy where Sq (A+B)

$$S_q(A_1 + \dots + A_n) = \sum_{i=1}^n S_q(A_i) + (1 - q) \sum_{i \neq j} S_q(A_i) S_q(A_j) + (1 - q)^2 \sum_{\substack{i \neq j \\ =s}} S_q(A_i) S_q(A_j) S_q(A_s) + \dots + (1 - q)^{n-1} \prod_{i=1}^n S_q(A_i) \quad (3)$$

The Tsallis entropy can be extended to the fields of image processing, because of the presence of the correlation between pixels of the same object in a given image. The correlations can be regarded as the long-range correlations that present pixels strongly correlated in luminance levels and space fulfilling. Let us assume that an image can be represented by gray levels L. The probabilities of pixels at level i is denoted by pi; so pi + p2 + ..... = 1. If the image is divided into two classes, CA and CB by a threshold at level t, where class CA consists of gray levels from 1 to t and CB contains the rest gray levels from t + 1 to L, the cumulative probabilities can be defined as:

$$\omega_A = \sum_{k=1}^t P_k, \quad \omega_B = \sum_{k=t+1}^L P_k$$

Therefore, the normalization of probabilities PA and PB can be defined as:

$$P^A = \{p_1, p_2, \dots, p_t\},$$

$$P^B = \frac{\omega_A}{\omega_B} \{p_{t+1}, p_{t+2}, \dots, p_L\},$$

Now, the Tsallis entropy for each individual class is defined as:

$$S_q^A = \frac{1 - \sum_{k=1}^t (p_k^A)^q}{q - 1},$$

$$S_q^B = \frac{1 - \sum_{k=1}^t (p_k^B)^q}{q - 1}$$

= Sq (A)+ Sq (B), the Tsallis entropy becomes a superextensive entropy where Sq (A + B) > Sq (A) + Sq (B). The generalization of the pseudo additivity rule to n mutually independent subsystems

A1, . . . , An is given by:

The task is to maximize the total Tsallis entropy between class CA and CB. When the value of Sq (t) is maximized, the corresponding gray-level t\* is regarded as the optimum threshold value:

$$t^* = \arg \max (S_q(t))$$

The optimal threshold is the gray level that maximizes equation f (t) = H0 + H1. This Kapur’s entropy criterion method tries to achieve a centralized distribution for each histogram-based segmented region of the image. This Kapur’s entropy criterion method has also been extended to multilevel thresholding and can be described as follows: The optimal multilevel thresholding problem can be configured as a m-dimensional optimization problem, for determination of m optimal thresholds for a given image [t1, t2, ...tm], where the aim is to maximize the objective function:

$$f(t_1, t_2, \dots, t_m) = H_0 + H_1 + H_2 + \dots + H_m \quad [16]$$

where

$$H_0 = - \sum_{i=0}^{t_1-1} \frac{P_i \ln P_i}{\Omega_0}, \quad \Omega_0 = \sum_{i=0}^{t_1-1} P_i \quad (8)$$

$$H_1 = - \sum_{i=t_1}^{t_2-1} \frac{P_i \ln P_i}{\Omega_1}, \quad \Omega_1 = \sum_{i=t_1}^{t_2-1} P_i \quad (9)$$

$$H_m = - \sum_{i=t_m}^{L-1} \frac{P_i \ln P_i}{\Omega_m}, \quad \Omega_m = \sum_{i=t_m}^{L-1} P_i \quad (10)$$

### 3. Edge Detection Based On Multilevel Thresholding

Thresholding is one of the powerful methods used for image edge detection. Edge detection seeks to define the boundary between two or several regions having relatively distinct gray level properties [18].

Let F be a grayscale image of size M × N and g (i, j) be the gray value of the pixel of

coordinates  $(i, j)$ . Denote  $G = \{0 \leq g_{\min}, \dots, g_{\max} \leq 255\}$  the set of all gray levels forming this image, where  $g_{\min}$  and  $g_{\max}$  are the lowest and the highest gray levels, respectively. The multilevel image thresholding involves

$$A(x, y) = \begin{cases} 1, & \text{if } g^{\min} \leq f(i, j) \leq t_1 \\ 2, & \text{if } t_1 < f(i, j) \leq t_2 \\ \vdots & \vdots \\ k, & \text{if } t_{k-1} < f(i, j) \leq t_k \\ k+1, & \text{if } t_k < f(i, j) \leq g_{\max} \end{cases} \quad (11)$$

The multilevel thresholding task can be seen as a global combinatorial optimization problem to determine the  $k$  optimal thresholds  $t_1^* < \dots < t_k^*$  that maximize the fitness function based on the Tsallis or the Kapur entropies. The optimization problem will be solved using classical and quantum genetic algorithms.

Once the  $(k+1)$ -levels matrix  $A$  is constructed we use it to determine the borders delimiting the  $(k+1)$  different homogeneous regions. To do this, we use an edge detection procedure based on the 8-neighbors connectivity window. This procedure gives rise to a binary matrix  $B$  showing the objects borders within the image. The edge detection procedure is described in the following algorithm.

Let  $B$  a null matrix with size  $M \times N$

For  $i = 1:M$

For  $j = 1:N$  Compute

$$\lambda_1 = |A(i, j) - A(i, j-1)| + |A(i, j) - A(i, j+1)|$$

$$\lambda_2 = |A(i, j) - A(i-1, j)| + |A(i, j) - A(i+1, j)|$$

$$\phi_1 = |A(i, j) - A(i-1, j-1)| + |A(i, j) - A(i+1, j+1)|$$

$$\phi_2 = |A(i, j) - A(i-1, j+1)| + |A(i, j) - A(i+1, j-1)|$$

$$\text{if } \lambda_1 + \lambda_2 = 0 \text{ or } \phi_1 + \phi_2 = 0$$

$$B(i, j) = 1$$

end

end

end

#### 4. Numerical Results and Discussion

In order to check the proposed method (Edge detection based on QGA) in this article and compare with the edge

dividing the set  $G$  into  $k+1$  categories by means of  $k$  thresholds  $t_1 < \dots < t_k$ . Regarding the category of pixels, a  $(k+1)$ -levels image  $A$  of the same size as  $F$  is created by assigning each pixel its label as follows:

detectors based on CQA, common gray level test images with different resolutions and sizes are detected by the quantum and classical edge detection respectively. On the other hand two different forms of entropy are used as a fitness function to demonstrate the important roles played by the optimal choosing of the fitness function in the CGA and QGA.

The performance of the proposed scheme is evaluated through the numerical results using MAT-LAB. Prior to the application of this algorithm, no pre-processing was done on the tested images. We apply the previous methods on 10 real-world images displaying different sizes. As shown in Figures (2)-(11), the charts of the test images and the average of run time for the classical methods and proposed scheme. It has been observed that the proposed edge detector works effectively for different gray scale digital images as compare to the run time of CGA and QGA detectors.

Image quality is a characteristic of an image that measures the perceived image degradation (typically, compared to an ideal or perfect image). Two parameters are there: First, MSE, it is defined as the squared difference between the original image and estimated image

$$MSE = \frac{1}{N} \sum_{j=1}^N (X - \hat{X})^2 \quad (12)$$

where  $X$  = original value,  $\hat{X}$  = stego value and  $N$  = number of samples.

Second, PSNR, Peak Signal-to-Noise Ratio, often abbreviated PSNR, is an engineering term for the ratio between the maximum possible power of a signal and the power of corrupting noise that affects the fidelity of its representation [19]. Because many signals have a very wide dynamic range, PSNR is usually expressed in terms of the logarithmic decibel scale.

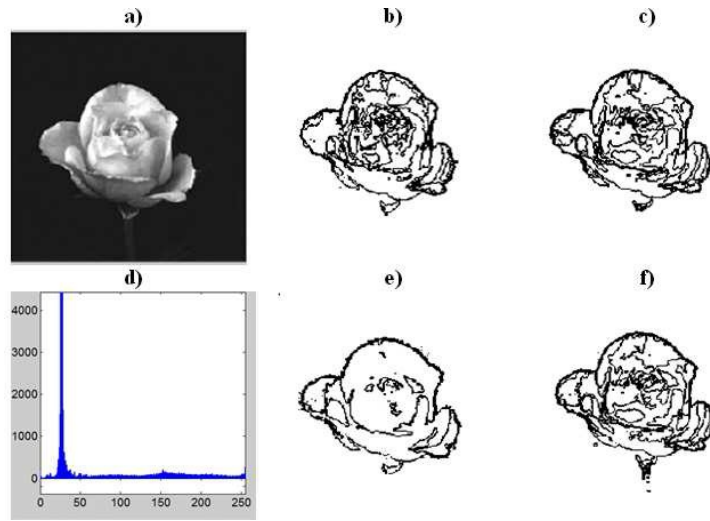


FIG. 3: (a) Original image 1, (b) CGA based on TE, (c) QGA based on TE, (d) Histogram, (e) CGA based on KE, (f) QGA based on KE.

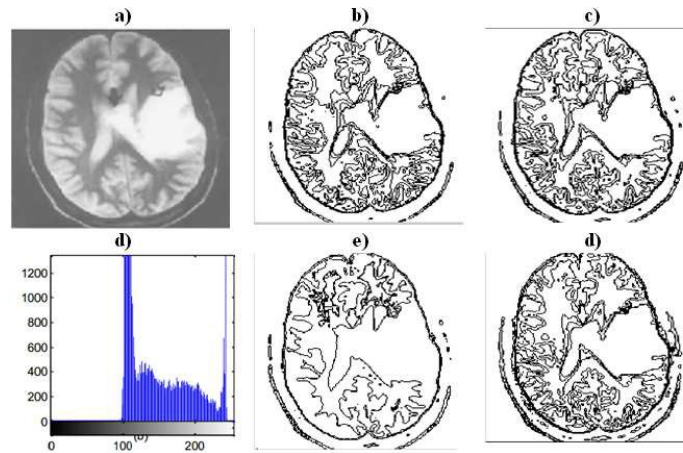


FIG. 4: (a) Original image 2, (b) CGA based on TE, (c) QGA based on TE, (d) Histogram, (e) CGA based on KE, (f) QGA based on KE.

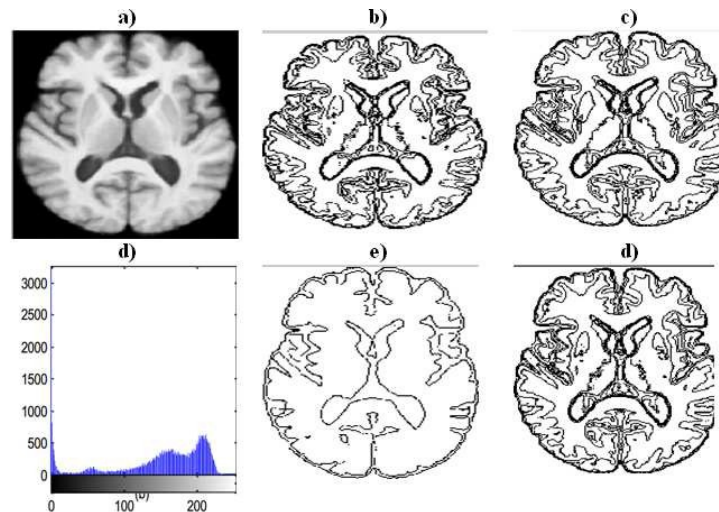


FIG. 5: (a) Original image 3, (b) CGA based on TE, (c) QGA based on TE, (d) Histogram, (e) CGA based on KE, (f) QGA based on KE.

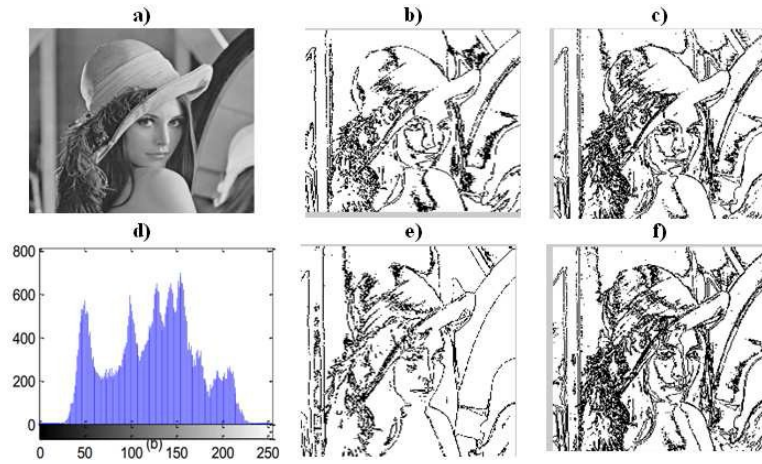


FIG. 6: (a) Original image 4, (b) CGA based on TE, (c) QGA based on TE, (d) Histogram, (e) CGA based on KE, (f) QGA based on KE.

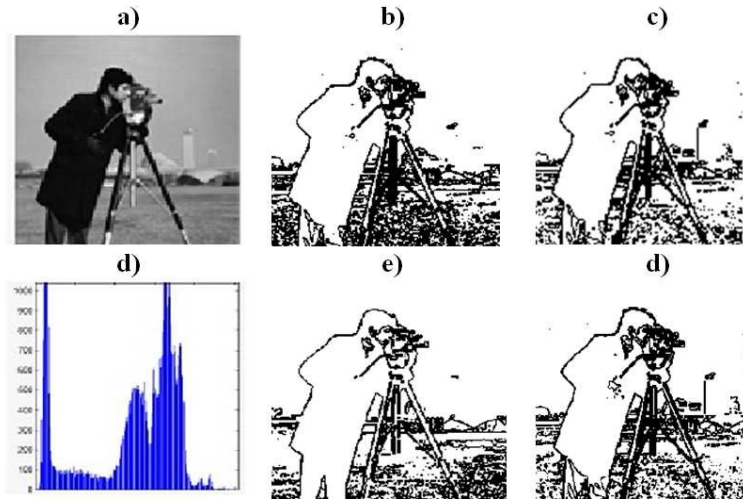


FIG. 7: (a) Original image 5, (b) CGA based on TE, (c) QGA based on TE, (d) Histogram, (e) CGA based on KE, (f) QGA based on KE.

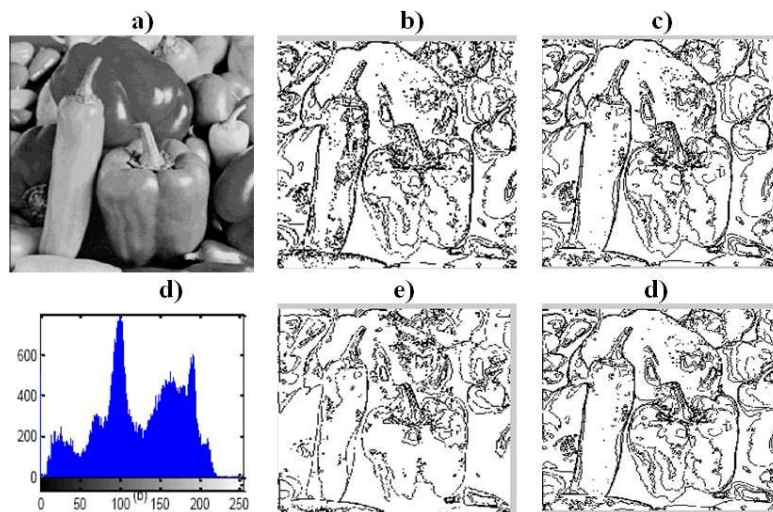


FIG. 8: (a) Original image 6, (b) CGA based on TE, (c) QGA based on TE, (d) Histogram, (e) CGA based on KE, (f) QGA based on KE.

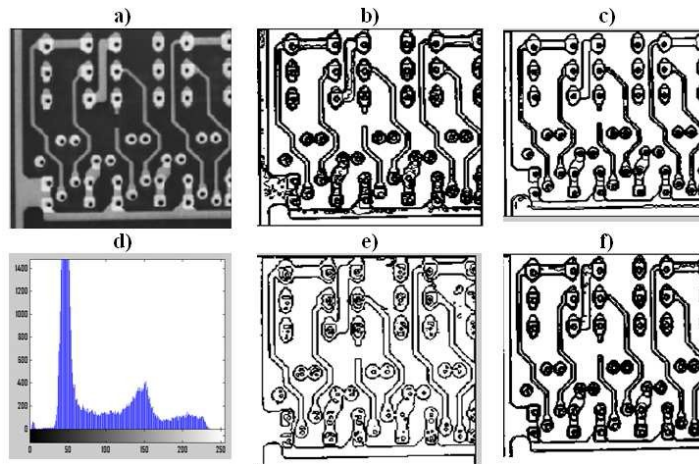


FIG. 9: (a) Original image 7, (b) CGA based on TE, (c) QGA based on TE, (d) Histogram, (e) CGA based on KE, (f) QGA based on KE.

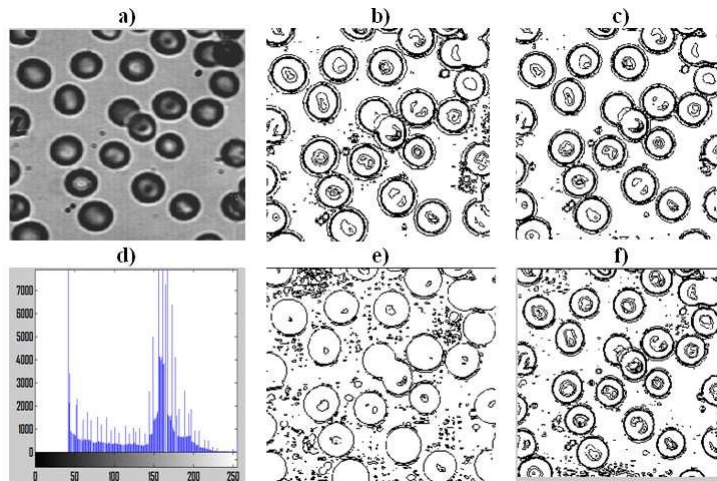


FIG. 10: (a) Original image 8, (b) CGA based on TE, (c) QGA based on TE, (d) Histogram, (e) CGA based on KE, (f) QGA based on KE.

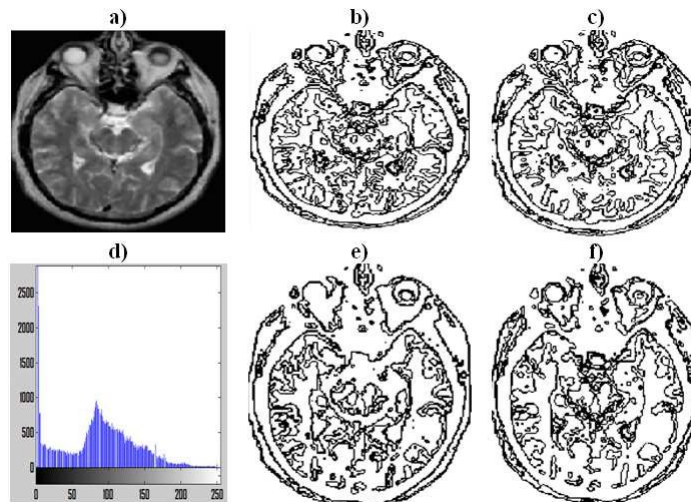


FIG. 11: (a) Original image 9, (b) CGA based on TE, (c) QGA based on TE, (d) Histogram, (e) CGA based on KE, (f) QGA based on KE.

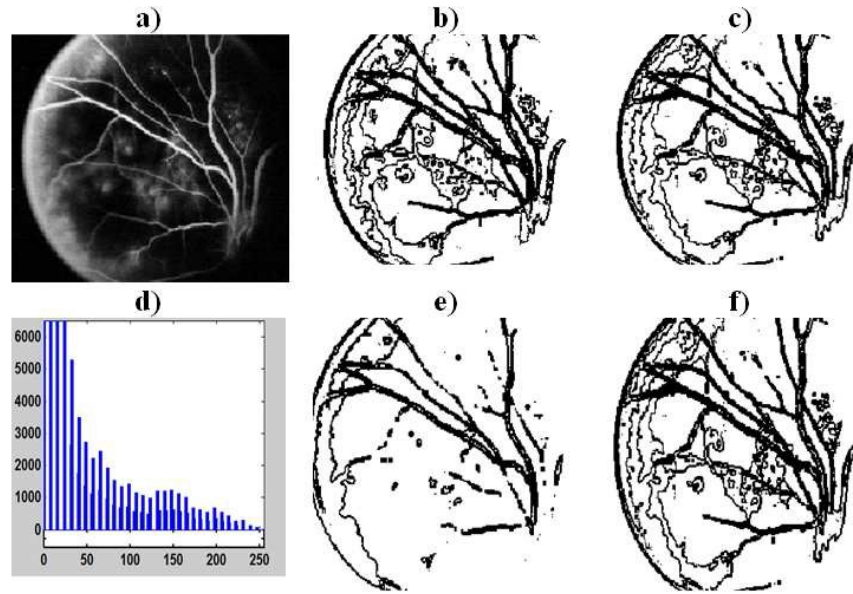


FIG. 12: (a) Original image 10, (b) CGA based on TE, (c) QGA based on TE, (d) Histogram, (e) CGA based on KE, (f) QGA based on KE.

Table 2: The numerical results on the ten images

| Image |               | PSNR        | Thresholds                 | Y               | Time         |
|-------|---------------|-------------|----------------------------|-----------------|--------------|
| Im.1  | <b>QGA TE</b> | <b>1.85</b> | <b>[52;101;151;203]</b>    | <b>19973.17</b> | <b>42.07</b> |
|       | CGA TE        | 1.84        | [44;111;174;199]           | 17459.22        | 16.47        |
|       | QGA KE        | 1.94        | [39;95;145;199]            | 17.54           | 29.75        |
|       | CGA KE        | 1.91        | [43;44;190;191]            | 10.81           | 13.76        |
| Im.2  | <b>QGA TE</b> | <b>5.86</b> | <b>[126;154;186;215]</b>   | <b>7487.47</b>  | <b>45.89</b> |
|       | CGA TE        | 5.75        | [128;161;199;225]          | 7155.33         | 23.69        |
|       | QGA KE        | 5.87        | [123;151;183;211]          | 16.01           | 37.59        |
|       | CGA KE        | 6.46        | [124;124;171;171]          | 10.76           | 21.83        |
| Im.3  | <b>QGA TE</b> | <b>4.19</b> | <b>[75;114;157;202]</b>    | <b>13543.06</b> | <b>47.26</b> |
|       | CGA TE        | 4.39        | [59;92;133;192]            | 12539.07        | 25.35        |
|       | QGA KE        | 4.17        | [82;120;157;198]           | 15.66           | 41.74        |
|       | CGA KE        | 3.78        | [177;180;200;200]          | 9.03            | 29.67        |
| Im.4  | <b>QGA TE</b> | <b>5.30</b> | <b>[71;110;148;185]</b>    | <b>18143.57</b> | <b>63.46</b> |
|       | CGA TE        | 5.26        | [57;112;164;201]           | 16212.14        | 43.26        |
|       | QGA KE        | 5.41        | [65;96;131;178]            | 17.99           | 57.53        |
|       | CGA KE        | 5.10        | [83;84;189;189]            | 11.98           | 20.45        |
| Im.5  | <b>QGA TE</b> | <b>4.95</b> | <b>[97; 142; 180; 209]</b> | <b>24461.66</b> | <b>54.57</b> |
|       | CGA TE        | 4.88        | [50;98;133;193]            | 23638.05        | 17.07        |
|       | QGA KE        | 4.94        | [44;97;146;195]            | 18.27           | 27.11        |
|       | CGA KE        | 4.93        | [77;77;114;114]            | 11.08           | 13.03        |
| Im.6  | <b>QGA TE</b> | <b>4.05</b> | <b>[59; 105; 148; 193]</b> | <b>21027.72</b> | <b>61.07</b> |
|       | CGA TE        | 3.87        | [60;106;151;188]           | 19806.47        | 23.25        |
|       | QGA KE        | 4.20        | [61;106;148;193]           | 18.19           | 45.79        |

|       |               |             |                         |                 |              |
|-------|---------------|-------------|-------------------------|-----------------|--------------|
|       | CGA KE        | 4.17        | [86;87;153;153]         | 12.20           | 29.86        |
| Im.7  | <b>QGA TE</b> | <b>3.02</b> | <b>[34;73;123;174]</b>  | <b>20782.48</b> | <b>38.49</b> |
|       | CGA TE        | 2.90        | [35;81;127;177]         | 20584.39        | 18.25        |
|       | QGA KE        | 3.25        | [34;61;119;171]         | 18.02           | 32.02        |
|       | CGA KE        | 3.81        | [55;60;103;105]         | 9.04            | 7.90         |
| Im.8  | <b>QGA TE</b> | <b>4.95</b> | <b>[97;142;180;209]</b> | <b>10217.56</b> | <b>54.57</b> |
|       | CGA TE        | 4.90        | [101;149;181;217]       | 9583.52         | 38.63        |
|       | QGA KE        | 4.93        | [97;144;179;208]        | 15.57           | 56.37        |
|       | CGA KE        | 4.67        | [179;183;207;208]       | 8.61            | 35.77        |
| Im.9  | <b>QGA TE</b> | <b>2.77</b> | <b>[84;131;180;215]</b> | <b>20653.78</b> | <b>36.39</b> |
|       | CGA TE        | 2.75        | [62;108;153;201]        | 19198.12        | 18.55        |
|       | QGA KE        | 2.64        | [92;128;180;215]        | 17.69           | 33.77        |
|       | CGA KE        | 2.38        | [126;126;187;189]       | 11.10           | 15.51        |
| Im.10 | <b>QGA TE</b> | <b>2.07</b> | <b>[40;89;149;207]</b>  | <b>170.02</b>   | <b>32.91</b> |
|       | CGA TE        | 1.92        | [48;106;166;215]        | 164.80          | 18.25        |
|       | QGA KE        | 2.07        | [40;89;141;190]         | 8.68            | 27.49        |
|       | CGA KE        | 1.99        | [40;40;157;157]         | 6.34            | 10.85        |

Table 2 shows the numerical results obtained on the ten real-world images. The first interesting result is that the QGA outperforms significantly the GA in the optimization task whatever the used entropy on all the used images. Indeed the achieved optimal value of the fitness function, denoted by Y, is usually higher when using the QGA. In the other hand, we see that the higher PSNR value corresponds to the higher optimal fitness value, except for image 3 when using the Tsallis entropy

and for images 2 and 7 when using the Kapur entropy. This agreement prove that achieving higher value for the fitness function leads to a better segmentation quality. Finally, the PSNR values obtained by QGA TE and QGA KE methods show that the Kapur entropy performs slightly better than the Tsallis entropy. Indeed, the PSNR values corresponding to QGA KE are higher on six from the ten images. This can be explained by the fact that Tsallis entropy based fitness function is more complex than that using the Kapur entropy.

## 5. Conclusion

In this work, we have presented a multilevel edge detection method based on Kapur and Tsallis entropies. We have employed CGA and QGA to solve the resulting optimization problem. It was proven that QGA is more efficient than CGA. Moreover, the Kapur entropy is cheaper to compute than the Tsallis one and gives rise to a better segmentation quality.

Of course, the problem of image segmentation remains one of the main open issues in image processing. Certainly this study deserves further methodological, algorithmic and numerical investigations. For instance, the QGA optimization performances can be improved by modifying the quantum gate and the population initialization. Furthermore, the fitness function maximization and the entropy parameter tuning, for each image, can be combined into a single optimization task. Finally, this work can be broadened by considering other entropies and a large sample of real-world and synthetic images.

## References

- [1] M. Tuba, Multilevel image thresholding by nature-inspired algorithms: A review, *Institute of Mathematics and Computer Science*, 22(3) 2014.
- [2] Y. Zhang and L. Wu, Optimal Multi-Level Thresholding Based on Maximum Tsallis Entropy via an Artificial Bee Colony Approach, *Entropy* (13) 2011.
- [3] Y. C. Liang and J. R. Cuevas, An Automatic Multilevel Image Thresholding Using Relative Entropy and Meta-Heuristic Algorithms, *Entropy* (15) 2013.
- [4] J. H. Holland, *Adaptation in Natural and Artificial Systems*, Cambridge, MA: MIT Press. Second edition (First edition, 1975).
- [5] J. H. Holland, Genetic algorithms. *Scientific American*, (1992).
- [6] S. Lou, Y. Li, Y. Wu, and X. Xiong, "Multi-objective reactive power optimization using quantum genetic algorithm," *High Voltage Engineering*, vol. 31, no. 9, pp. 69–83, 2005.
- [7] K. Liu and Z. Q. Zhu *IEEE Transactions on Industry* 62, 2015
- [8] X. k. Wei, W. Shao, C. Zhang and J. Li, *IET Microwaves, Antennas & Propagation*, 8, pp. 965 - 972, 2014.
- [9] U. Roy, S. Roy and S. Nayek, *International Journal of Computer Applications*, 102, pp.1-7, 2014. [10] G. X. Zhang, N. Li, and W. D. Jin, "A novel quantum genetic algorithm and it's application," *Acta Electronica Sinica*, vol. 32, no. 3, pp. 476–479, 2004.
- [10] G. Zhang and H. Rong, "Quantum-inspired genetic algorithm based time-frequency atom decomposition," in *Proceedings of the 7th International Conference on Computational (ICCS '07)*, pp. 243–250, 2007.
- [11] J.-A. Yang and Z.-Q. Zhuang, "Actuality of research on quantum genetic algorithm," *Journal of Computer Science & Technology*, vol. 30, no. 11, pp. 13–15, 2000
- [12] N. H. Abbasy and H. M. Ismail, "A unified approach for the optimal PMU location for power system state estimation," *IEEE Transactions on Power Systems*, vol. 24, no. 2, pp. 806–813, 2009
- [13] H. Wang, J. Liu, J. Zhi and C. Fu, "The Improvement of Quantum Genetic Algorithm and Its Application on Function Optimization," *Mathematical Problems in Engineering*, 2013, Article ID 730749, 10, 2013.
- [14] W. Shu and B. He, "A quantum genetic simulated annealing algorithm for task scheduling," in *Advances in Computation and Intelligence*, vol. 4683 of *Lecture Notes in Computer Science*, pp. 169–176, 2007.
- [15] Guida, A.; Nienow, A.W.; Barigou, M. Shannon entropy for local and global description of mixing by Lagrangian particle tracking. *Chem. Eng. Sci.* 2010, 65(10), 2865–2883.
- [16] S. P. Duraisamy and R. Kayalvizhi, *J. Intelligent Learning Systems & Applications* 2, pp. 126-138, 2010.
- [17] A. S. Ashour, M. A. El-Sayed, S. E. Waheed and S. Abdel-Khalek, *New Method Based on Multi-Threshold of Edges Detection in Digital Images*, *IJACSA* 5(2) 2014.
- [18] S. Jayaraman, S. Esakkirajan and T. Veerakumar, "Digital Image Processing," *Tata McGraw Hill Education ptd. Ltd*, New Delhi, 7th ed., 2012, pp.368-393.